

Optical properties of homotropically oriented nematic-crystal elliptically deformed nematic crystal layer

O. A. Kapustina, E. H. Kozhevnikov,¹⁾ and G. N. Yakovenko

Acoustics Institute, USSR Academy of Sciences

(Submitted 26 December 1983; resubmitted 3 May 1984)

Zh. Exp. Teor. Fiz. **87**, 849–858 (September 1984)

A new effect was observed, viz., stationary distortion of a homotropically oriented elliptically deformed crystal. This effect is produced when the layer is simultaneously acted upon by periodic shear and compression deformation at low sound frequencies, when the viscous wavelength exceeds considerably the layer thickness. This effect is not connected with the action of previously known mechanisms (velocity gradients, electric or magnetic field) but is due to nonlinear interaction between the director oscillations and the velocity field. It is shown that the presence of even small ellipticity of plate motion (ratio of transverse and longitudinal amplitudes $\beta = 10^{-3}$) leads to a significant stationary effect. An adequate description of the effect can be obtained only if account is taken of the nonlinear interactions of the director oscillations with the velocity field. In the limiting case $\beta = 0$ the mode describes the polarizational modulation of light in shear deformation of a homotropically oriented nematic liquid crystal.

INTRODUCTION

We have investigated theoretically and experimentally the optical properties of a homotropically oriented layer of an elliptically deformed nematic liquid crystal (NLC). This layer deformation is produced by simultaneous action of periodic compression and shear strains of equal frequency but shifted in phase. We considered a frequency band in which the viscous wavelength exceeded considerably the sample system. The optical properties of an NLC layer are determined by the director motion, which is described in the case of elliptic deformation within the framework of NLC hydrodynamics with inclusion of the quadratic terms in the equations for the director and of the motion. We shall show that nonlinear effects lead to a time-averaged tilt of the director away from the normal, so that it oscillates about a new quasi-equilibrium position. The stationary effect is due mainly to the action of nonlinear moments and decreases somewhat by the liquid flow. This stationary tilt of the director at acoustic frequencies is of different nature than the effects observed at ultrasonic frequencies, when the molecule rotation is due to acoustic fluxes. We construct a theory of the optical properties of an elliptically deformed NLC layer and compare the calculation results with the experimental data.

The results reveal a new mechanism of stationary distortion of the structure of an NLC layer, a mechanism connected with nonlinear interaction between the director vibrations and the velocity field, and is important for a correct interpretation of the data previously obtained¹⁻³ for shear-deformed NLC in different laboratories at acoustic frequencies. The point is that the theoretical analysis of the optical behavior of the samples is usually carried out within the framework of linear hydrodynamics, which yields a director rotation angle $\varphi \approx (\xi_0/d) \sin \omega t$ and leads to a layer optical transparency that does not depend on the oscillation frequency^{3,4} (here d is the layer thickness, ξ_0 and ω the oscillation frequency and amplitude, and t the time). This conclusion contradicts the results of experiments in which the observed optical transparency exceeds the theoretical al-

ready at several times ten hertz and depends on the oscillation frequency.¹⁻³ It follows from further analysis that the discrepancy can be explained by recognizing that in all the known experiments the layer was compressed by the "parasitic" transverse component of the motion of the plates enclosing the layer, i.e., what actually took place was the elliptic deformation not taken into account by the linear hydrodynamic theory.

THEORY

Consider two-dimensional deformation of a homotropically oriented NLC layer with free ends in a coordinate frame with the origin ($x = 0, z = 0$) at the center of its lower boundary and with the z axis perpendicular to the layer. The motion of the liquid and the rotation of the molecules take place in the xz plane. The external action is specified by the motion of the upper boundary of the layer, in the form

$$v_x|_{z=d} = v_0 \cos \omega t, \quad v_z|_{z=d} = \beta v_0 \sin \omega t, \quad (1)$$

where v_0 and βv_0 are the amplitudes of the longitudinal and transverse components of the boundary velocity. The lower boundary is immobile. We confine ourselves to frequencies at which the following inequalities hold:

$$K_3/\eta d^2 \ll \omega \ll \eta/\rho d^2 \quad (1a)$$

(the length of the viscous wave in the NLC is larger and that of the orientational wave smaller than the NLC layer thickness);

$$\eta/\rho L^2 \ll \omega \ll c/L \quad (1b)$$

(the sound wavelength is larger and the viscous wavelength is smaller than the layer length L). Here ρ is the density, η the viscosity, c the speed of sound in the NLC layer, and K_3 is the Frank elastic constant. The first of these conditions allows us to neglect the effect of the layer boundaries in the calculation of the periodically varying molecule-rotation angle and to discard the elastic terms in the equation for the director. The second allows us to assume that the compressed NLC layer behaves as an incompressible liquid. We assume in ad-

dition that the NLC satisfies the natural condition $L \gg d$. The calculation will be carried out for small molecule rotation angles, to permit linearization, with respect to the angle, of the viscous stresses in the equation of motion of the liquid and the moments in the equation for the director.

The layer compression by low-frequency vibrations of its upper boundaries in the direction normal to the layer causes the incompressible liquid to spread towards the open ends at a velocity having a profile

$$v_x = \text{const} \cdot x(z^2 - zd) \sin \omega t.$$

By determining the velocity v_z in terms of v_x from the incompressibility condition ($\text{div } \mathbf{v} = 0$), and the constant from the boundary conditions for v_z , as well as taking into account the velocity $v_x = v_0(z/d) \cos \omega t$ due to the displacement of the upper plate in its own plane, we obtain for the velocity distribution that satisfies condition (1) in a layer the following expressions:

$$\begin{aligned} v_x &= v_0 \frac{z}{d} \cos \omega t + 6\beta v_0 \frac{x(z^2 - zd)}{d^3} \sin \omega t, \\ v_z &= -\beta v_0 \frac{2z^3 - 3z^2 d}{d^3} \sin \omega t. \end{aligned} \quad (2)$$

The equation for the small molecule rotation angle, with allowance for the second-order terms, is

$$\begin{aligned} \gamma_1 \frac{\partial \varphi}{\partial t} - K_3 \Delta \varphi \\ = -\alpha_2 \frac{\partial v_x}{\partial z} - \alpha_3 \frac{\partial v_z}{\partial x} - \gamma_1 (\mathbf{v} \nabla) \varphi - \gamma_2 \varphi \left(\frac{\partial v_x}{\partial x} - \frac{\partial v_z}{\partial z} \right), \end{aligned} \quad (3)$$

where $\gamma_1 = \alpha_3 - \alpha_2$; $\gamma_2 = \alpha_3 + \alpha_2$; α_i are the Leslie viscosity coefficients.⁵ In the calculations that follow the small viscosity coefficients α_1 and α_3 are set equal to zero, and $\gamma_1 = -\gamma_2 = -\alpha_2 = \gamma$.

In first approximation, neglecting the influence of the layer boundaries and taking Eqs. (2) into account, we get

$$\varphi_1 = (\xi_0/d) \sin \omega t - [6\beta \xi_0 x(2z - d)/d^3] \cos \omega t, \quad \xi_0 = v_0/\omega.$$

The second approximation in (3) leads to an equation for the time-averaged molecule-rotation angle φ_2 :

$$K_3 \Delta \varphi_2 = \gamma \left\{ \langle (\mathbf{v} \nabla) \varphi_1 \rangle + \left\langle \varphi_1 \left(\frac{\partial v_x}{\partial z} - \frac{\partial v_z}{\partial x} \right) \right\rangle - \frac{\partial v_{xz}}{\partial z} \right\},$$

where v_{xz} is the velocity of the stationary flow in the layer. We obtain the equation for v_{xz} by eliminating the pressure from the NLC equations of motion and discarding small quantities of order $(\partial/\partial x/\partial/\partial z)^2 \sim d^2/L^2 \ll 1$:

$$\eta_2 \frac{d^3 v_{xz}}{dz^3} = \gamma \frac{d^2}{dz^2} \left[\langle (\mathbf{v} \nabla) \varphi_1 \rangle + \left\langle \varphi_1 \frac{\partial v_x}{\partial z} \right\rangle \right],$$

where $\eta_2 = (\alpha_1 + \alpha_5 - \alpha_2)/2$ and the angle brackets $\langle \dots \rangle$ denote averaging over the period $2\pi/\omega$. The first term in the right-hand side of the equation for φ_2 describes the transport of the molecule rotation to the center of the layer from its edges, where the rotation angle due to the spreading of the liquid upon compression of the layer is a maximum. The second term describes the molecule rotation supplementing those due to "pure shear" upon compression or dilatation of the layer: molecule rotation due to shear increases somewhat in one direction when the liquid simultaneously contracts

along the z axis and expands along x . Conversely, rotation in the other direction decreases somewhat when the liquid expands along z and contracts along x . As a result a cumulative rotation of the molecules occurs after each period of elliptic deformation. These effects decrease somewhat the stationary flows.

We solve the equation for v_{xz} under conditions when the NLC is anchored to the boundaries:

$$v_{xz}|_{z=0} = v_{xz}|_{z=d} = 0$$

and the flow is closed:

$$\int_0^d v_{xz} dz = 0.$$

We determine the boundary conditions for φ_2 with allowance for the finite bonds of the NLC molecules to the surfaces that confine the NLC. Assuming a surface orienting energy density in the form $F_s = (1/2)\omega\varphi^2$, we arrive at the boundary conditions:

$$w\varphi - K_3 \frac{\partial \varphi}{\partial z} \Big|_{z=0} = 0, \quad w\varphi + K_3 \frac{\partial \varphi}{\partial z} \Big|_{z=d} = 0.$$

Solution of the stationary equation under the indicated boundary conditions leads to the following expression:

$$\begin{aligned} \varphi_2 = {}^{1/2} \beta \gamma \omega \xi_0^2 K_3^{-1} d^{-4} \{ -[2z^4 - 3z^3 d + z d^3 - \delta z d^3 / (1+2\delta) \\ + \delta(1+\delta)d^4 / (1+2\delta)] + {}^{3/2} \gamma \eta_2^{-1} (z^4 - 2z^3 d + z^2 d^2) \}, \end{aligned}$$

where the dimensionless parameter $\delta = K_3/\omega d$ determines the degree of bonding of the molecules with the boundary; its limiting values $\delta \gg 1$ and $\delta \ll 1$ correspond to weak and strong bonds.

The model of the behavior of the director for elliptic deformation of an NLC layer is shown schematically in Fig. 1. Each point of the moving plate describes an ellipse in the xz plane; ξ_0 and $\beta\xi_0$ are the amplitudes of the longitudinal and transverse vibrations of this plate.

The optical transparency of the sample viewed through crossed polarizers, with allowance for the variation of the molecule orientations over the layer thickness, is given by⁶

$$m = \frac{I}{I_0} = \sin^2 \left[\frac{k_0 \Delta n}{2} \int_0^d \varphi^2 dz \right] \sin^2 2\psi, \quad (4)$$

where I_0 and I are the intensities of the light passing through the first and second polarizers; $\Delta n = n_{\parallel} - n_{\perp}$; n_{\parallel} and n_{\perp} are the refractive indices along and perpendicular to the crystal optical axis, k_0 is the wave number of the light in the ordinary wave, and ψ is the angle between the light polarization plane and the shear direction (the x axis). Substituting in (4) the total molecule rotation angle $\varphi = \varphi_1 + \varphi_2$, we get

$$m = m(t) = \sin^2 [(P_0 + P_1 \sin \omega t - P_2 \cos 2\omega t)/2] \sin^2 2\psi, \quad (5)$$

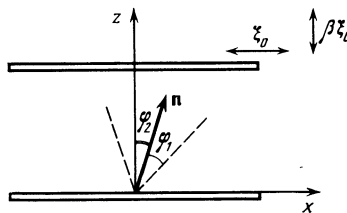


FIG. 1. Model of behavior of director \mathbf{n} under elliptic deformation.

where

$$\begin{aligned}
 P_0 &= 0.0075 \Delta n k_0 d (\beta \gamma \omega \xi_0^2 K_3^{-1})^2 \\
 &\quad \times [1 + 0.12 \gamma^2 \eta_2^{-2} - 0.67 \gamma \eta_2^{-1} + f(\delta)] \\
 &\quad + \frac{1}{2} \Delta n k_0 \xi_0^2 d^{-1} (1 + 12 \beta^2 x^2 d^{-2}), \\
 P_1 &= -0.15 \Delta n k_0 \beta \gamma \omega \xi_0^3 K_3^{-1} (1 - 0.33 \gamma \eta_2^{-1} + 3.33 \delta), \\
 P_2 &= \frac{1}{2} \Delta n k_0 \xi_0^2 d^{-1} (1 - 12 \beta^2 x^2 d^{-2}), \\
 f(\delta) &= [5.5 (1 + 2\delta)^{-1} - 1.65 \gamma \eta_2^{-1}] \delta \\
 &\quad + 11 \delta^2 (1 + 3\delta + 3\delta^2) (1 + 2\delta)^{-2}.
 \end{aligned} \tag{6}$$

We confine ourselves next to an analysis of the effect in the central part of the layer at low values of β . Then, discarding the terms proportional to $\beta^2 x^2 / d^2$ in the expressions for P_0 and P_2 and assuming that $12 \beta^2 x^2 / d^2 \ll 1$ we get

$$\begin{aligned}
 P_0 &= 0.0075 \Delta n k_0 d (\beta \gamma \omega \xi_0^2 / K_3)^2 [1 + 0.12 (\gamma / \eta_2)^2 \\
 &\quad - 0.67 \gamma / \eta_2 + f(\delta)] + \Delta n k_0 \xi_0^2 / 2d, \\
 P_2 &= \Delta n k_0 \xi_0^2 / 2d.
 \end{aligned} \tag{7}$$

The transparency $m(t)$ has a periodic time dependence with period $2\pi/\omega$. To analyze the result, we represent $m(t)$ as a Fourier expansion:

$$m(t) = m_0 + \sum_{k=1}^{\infty} m_k \cos(k\omega t + \alpha_k),$$

where m_0 and m_k are the spectral amplitudes of the Fourier expansion and α_k is the phase lag relative to the shear vibrations of the plate.

It follows from (5) and (6) that in the general case the transparency is determined both by linear and nonlinear hydrodynamic effects. At low d , ω , and ξ_0 , which satisfy the inequality

$$0.1 \gamma \beta \omega \xi_0 d / K_3 \ll 1,$$

the nonlinear effects are small and the equation for the transparency is

$$m = \sin^2 [\frac{1}{2} P_2 (1 - \cos 2\omega t)] \sin^2 2\psi. \tag{8}$$

In this case the intensity of the light passing through the second polarizer has a dc component $m_0 I_0$ and an ac component $m_{2n} I_0$ which is a sum of even harmonics, where

$$m_0 = \frac{1}{2} [1 - J_0(P_2) \cos P_2] \sin^2 2\psi, \tag{9a}$$

$$m_{2n} = -\frac{1}{2} J_{2n}(P_2) \cos P_2 \sin^2 2\psi, \tag{9b}$$

and J_0 and J_{2n} are Bessel functions of first order.

The values of m_0 and m_{2n} are determined only by the parameter P_2 and do not depend on the frequency. The dc component of m_0 is proportional at $P_2 \ll 1$ to the ratio ξ_0^4 / d^2 ; with increasing P_2 , m_0 increases and reaches at $P_2 = 1.97$ to first maximum $m_{0\max} = 0.55$; with further increase of P_2 the value of m_0 oscillates about $m_0 = 0.5$. The component m_2 reaches its first maximum $m_{2\max} \approx 0.3$ at $P_2 = 1.2$, and also oscillates with increasing P_2 . The first maxima of the functions J_{2n} shift with increasing n towards larger values of the argument, so that the maximum values of the harmonics m_{2n} ($n \geq 2$) shift towards larger amplitudes with increasing number n .

At high frequencies and amplitudes, when the inequality $0.1 \beta \omega d \xi_0 / K_3 \gg 1$ holds, the transparency is determined by the nonlinear effects and Eq. (5) takes the form

$$m = \sin^2 (\frac{1}{2} P_0 + \frac{1}{2} P_1 \sin \omega t) \sin^2 2\psi, \tag{10}$$

where $P_0 > P_1$. The spectrum of the optical signal is represented in this case by both even and odd harmonics:

$$m_0 = \frac{1}{2} [1 - J_0(P_1) \cos P_0] \sin^2 2\psi, \tag{11a}$$

$$m_n = -\frac{1}{2} J_n(P_1) \cos P_0 \sin^2 2\psi, \quad n=1, 2, 3 \dots \tag{11b}$$

At $P_0 \gg P_1$ the first maximum of the static component corresponds to the condition $P_0 \approx \pi$; the position of the principal (largest) maximum of the harmonics m_n can be estimated from the condition that the function $J_n(P_1)$ reach its first maximum. Consequently, in the nonlinear region the first maximum of the static component of the optical signal should be observed at shear amplitudes ξ_0 smaller than the principal maxima m_n of the harmonics.

The results are valid at small molecule rotation angles $\varphi \ll 1$ and if conditions (1a) and (1b) are met by ω . These angles are small in the linear region of the effect, at real displacement amplitudes $\xi_0 \lesssim 10^{-4}$ cm and layer thicknesses $d \gtrsim 10 \mu\text{m}$. Estimating the maximum values of the angle φ_2 in the nonlinear region, at $\delta < 1$ and $3/2 \gamma \eta_2^{-1} \approx 1$, we arrive at the condition $0.7 (P_0 / \Delta n k_0 d)^{1/2} < 1$. At the first maximum of the static component of the optical signal in the nonlinear region ($\xi_0 = \xi_{0\max}$, $P_0 \approx \pi$) this condition takes at $\Delta n \approx 0.2$ and $k_0 = 1.5 \cdot 10^5 \text{ cm}^{-1}$ the form $d > d_{\min} \approx 0.5 \mu\text{m}$. As ξ_0 increases this condition is violated at amplitudes $\xi_0 > \xi_{0\max} (d / d_{\min})^{1/4}$.

EXPERIMENT

The experiments were performed with a setup similar to that described in Ref. 7. The samples were made of a mixture of MBBA and EBBA between plane-parallel glass plates. One plate was immobile and the other, connected to an electrodynamic vibrator, could vibrate in its own plane and in a direction perpendicular to it. The longitudinal and transverse components of these motions were recorded with contact accelerometers connected to vibrometers. The ratio of the vibration phases was monitored with a phase meter. The intensity of the light flux passing through the polarizer + NLC layer + analyzer system was recorded with a photomultiplier connected to a dc voltmeter and a spectrum analyzer. The light source was an He-Ne laser. The thickness of the NLC sample ranged in the experiments from 10 to 100 μm , the frequency range was 7–1500 Hz, and the ratio β of the amplitudes of the transverse and longitudinal components of the motion ranged from 0.001 to 0.9. Homotropic orientation of the NLC molecules in the layer was ensured by introduction of lecithin.

EXPERIMENTAL RESULTS AND DISCUSSION

It follows from the theory that the spectral composition of an optical signal depends on the quantity $l = 0.1 \gamma \beta \omega d \xi_0 / K_3$; at $l \ll 1$ it contains only even harmonics, whereas at $l > 1$ it contains also odd ones. This confirms the oscillograms of the optical and acoustic signals shown in Fig. 2. The change of the spectrum (Figs. 2a,b) points to the appearance of a sta-

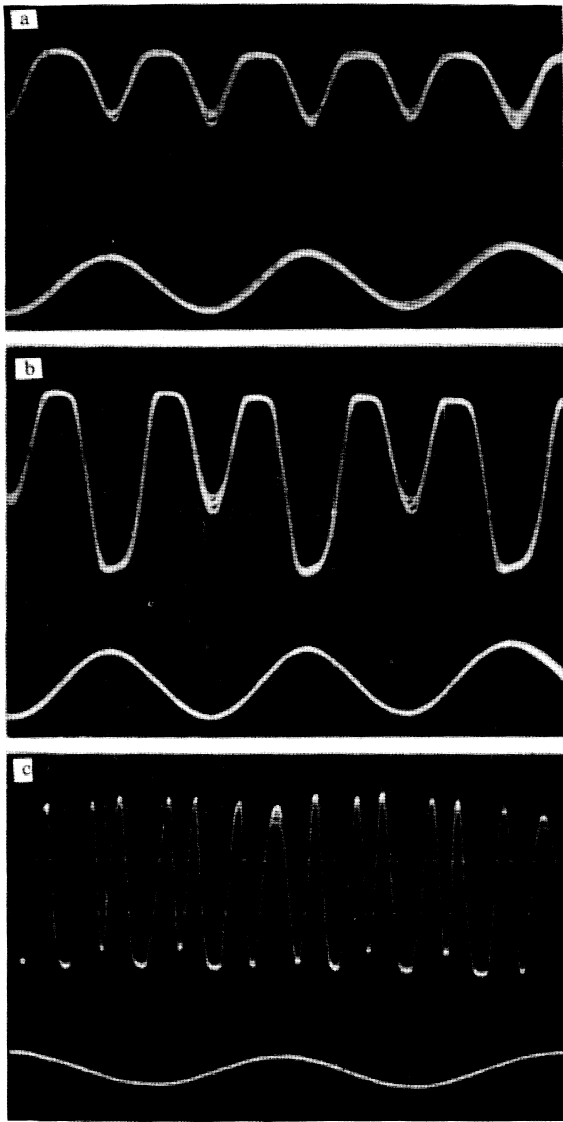


FIG. 2. Oscillogram of optical (upper traces) and acoustic (lower traces) of signals obtained at the following values: a) $l = 0.14$, $d = 100 \mu\text{m}$, $f = 49$ Hz; b) $l = 3$, $d = 100 \mu\text{m}$, $f = 49$ Hz; c) $l = 9.6$, $f = 82$ Hz, $\beta = 25 \cdot 10^{-3}$, $d = 50 \mu\text{m}$.

tionary distortion of the layer structure on going through the critical value $l = 1$, when the director now oscillates about

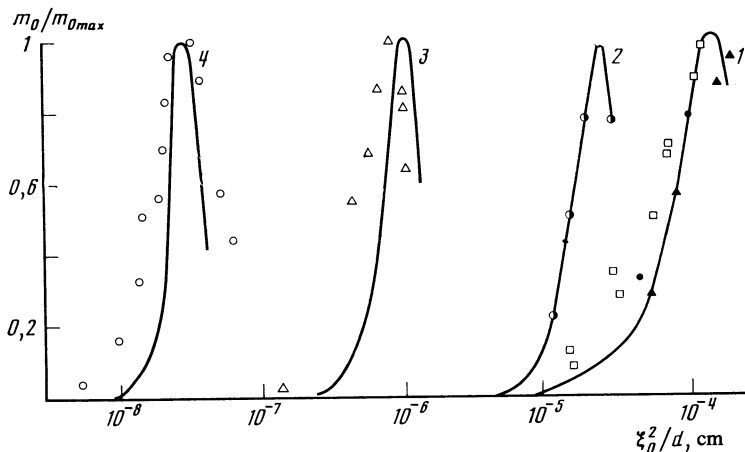


FIG. 3. Dependence of the static component of the optical signal on the ratio ξ_0^2/d . Linear region: experimental data — \square ($d = 37.5 \mu\text{m}$, $f = 40$ Hz), \bullet ($d = 25 \mu\text{m}$, $f = 70$ Hz) and \blacktriangle ($d = 25 \mu\text{m}$, $f = 40$ Hz); theory—curve 1. Nonlinear region: experimental data— \circ ($d = 15 \mu\text{m}$, $f = 32$ Hz, $\beta = 0.1$), \triangle ($d = 100 \mu\text{m}$, $f = 416$ Hz, $\beta = 0.04$) and \circ ($d = 50 \mu\text{m}$, $f = 1468$ Hz, $\beta = 0.9$); theory—curves 2-4. 1 — $l_0 = 0$; 2 — $l_0 = 0.8$; 3 — $l_0 = 15$; 4 — $l_0 = 70$.

the “quasi-equilibrium” position defined by the angle φ_2 (see Fig. 1). With increasing l this angle increases and the numbers of the harmonic components present in the optical signal increase (Fig. 2c).

In Figs. 3 and 4 are compared the theoretically obtained static component of the optical signal with the experimental data, for different d , β , and f . Figure 3 shows the experimental data and the theoretical curves for the static transparency component m_0 within the limits of the first maximum as functions of ξ_0^2/d . Specifying the displacement in the form of the combination ξ_0^2/d permits separation of the linear region of the effect, where the optical signal is determined by this quantity only. To compensate for the variation of the light-source intensity from experiment to experiment, m_0 is normalized to the maximum transparency $m_{0\text{max}}$. Curve 1 is a plot of Eq. (19a) corresponding to the value $\beta = 0$ and describing the static component of the optical transparency of the layer under shear deformation. Curves $p-4$, shifted towards lower amplitudes, were calculated for the corresponding values of the parameters by numerically averaging Eq. (5) over the vibration period $2\pi/\omega$. The NLC parameters assumed in the calculations were those for MBBA, viz., $K_3 = 7 \cdot 10^{-7}$ dyn, $\gamma = 0.78$ P, $\eta_2 = 1.14$ P, and $\Delta n = 0.2$ (Ref. 5). The wave number of the light was assumed to be $k_0 = 1.5 \cdot 10^5 \text{ cm}^{-1}$. The value of w was chosen to obtain agreement between theory and experiment at small layer thicknesses, when the bond between the NLC molecules and the bounding surfaces cannot be regarded as strong. The chosen value $w = 10^{-3}$ erg/cm agrees in order of magnitude with the experimental values of w for a surface treated with lecithin.⁸ The parameter that determines the degree of nonlinearity of the effect is chosen to be the value of l at the amplitude corresponding to the maximum transparency at given d and f , viz. $l_0 = l(\xi_{0\text{max}})$. Curve 1 agrees well with the experimental data corresponding to small ellipticity, when $l_0 \ll 1$. In the nonlinear region ($l_0 > 1$) the experimental data corresponding to $l_0 = 0.8, 15$, and 70 also correlate with the theoretical curves that describe the change of the sample transparency under elliptic deformation. The same regularities appear also for the alternating component of the optical signal.⁹

We proceed now to analyze the frequency dependence of the effect under elliptic deformation. Figure 4 shows, as

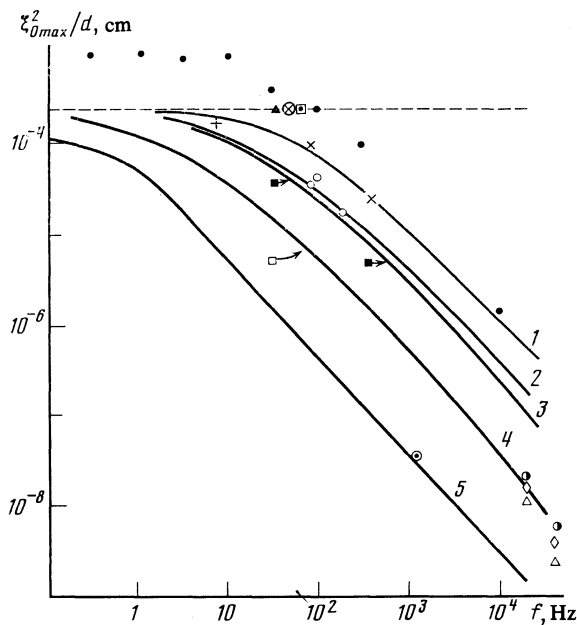


FIG. 4. Frequency dependence of the static component of the optical signal. Linear region: experimental data— \blacktriangle ($d = 37.5 \mu\text{m}$), \otimes ($d = 75 \mu\text{m}$), \square ($d = 25 \mu\text{m}$), $+$ ($d = 60 \mu\text{m}$); theory—dashed line. Nonlinear region: experimental data— \otimes ($d = 15 \mu\text{m}$, $\beta = 0.02$), \circ ($d = 50 \mu\text{m}$, $\beta = 0.01$), \blacksquare ($d = 15 \mu\text{m}$, $\beta = 0.1$), \square ($d = 50 \mu\text{m}$, $\beta = 0.08$), \odot ($d = 50 \mu\text{m}$, $\beta = 0.9$); theory—curves 1–5 corresponding to the indicated values of d and β . Data of Ref. 2— \bullet ($d = 55 \mu\text{m}$) and of Ref. 1— \circ , \diamond , \triangle respectively $d = 66, 105,$ and $155 \mu\text{m}$.

functions of frequency, the theoretical curves and the experimental data for the squared amplitude of the displacement corresponding to the first maximum of the function $m_0(\xi_0)$, divided by the layer thickness: $U = \xi_{0\max}^2/d$. Here, too, the theory correlates well with the experimental data. At low frequencies, when $l_0 \ll 1$, the experimental values of U are independent of f and are close to the theoretical $U = 1.31 \cdot 10^{-4}$ cm. Raising the vibration frequency and shifting to the region $l_0 > 1$ decreases U more the larger β , d , and f . At $l_0 > 1$ the frequency dependence of $\xi_{0\max}$ takes the form $\xi_{0\max} \sim f^{-1/2}$.

These regularities are illustrated by the experimental results in the frequency range 7–1500 Hz. To establish a correlation between theory and experiment in a wider range of frequencies, we analyzed the data of Ref. 2 on the variation of the transparency of MBBA samples of thickness 55 μm under shear deformation at frequencies 0.1 Hz–21 kHz, as well as the data of Ref. 1 for layer thicknesses 66, 105, and 153 μm at the frequencies 23.3 and 45.2 kHz. These data are also marked in Fig. 5. Their analysis shows that the data of Ref. 2 correspond to “pure shear” only at frequencies $f < 10$ Hz; on the other hand, the decrease of U with further increase of frequency is in full agreement with the changes that

follow from the proposed model of elliptic deformation with low ellipticity. This allows us to conclude that “parasitic” movable-plate vibrations that compressed the NLC layer took place in Ref. 2 and but were not taken into account by its author.

At several tens of kilohertz, when the length of the viscous wave is shorter than d , the shear is no longer uniform over the layer thickness. In this case the entire effect evolves within a layer whose thickness is of the order of the length of the viscous wave. The experimental values of $\xi_{0\max}$ are then lower than predicted by the theory and do not agree qualitatively with its premises. Thus, in Ref. 1 the values of $\xi_{0\max}$ at 23.3 kHz and for samples 66, 105, and 153 μm thick are respectively 0.13, 0.18, and 0.15 μm , i.e., practically independent of the layer thickness. This behavior takes place at 45.2 kHz. The same remark applies also to the data of Ref. 2 at 21 kHz. This discrepancy between theory and experiment can be explained by assuming that in these experiments the sample was also compressed, and the observations were made not at the center of the layer. A major role in the effect should be played in this case by the spreading of the liquid in the layer located next to the vibrating plate and having a thickness of the order of the length of the viscous wave; the parameter P_2 in the linear region can be estimated at

$$P_2 \sim 1/2 \Delta n k_0 q^2 x^2 \xi_0^2 \beta^2, \quad (12)$$

where $q = (\rho\omega/2\eta)^{1/2}$ is the wave number of the viscous wave and η is the shear viscosity.

It follows from a comparison of (6) and (12) that at high frequencies, at $\beta \sim 1$ and $x \sim 1$ cm, the linear effect is stronger than the quadratic one considered above; in this case $\xi_{0\max}$ does not depend on the layer thickness. However, the lack of detailed data on the experiments described in Refs. 1 and 2 prevents a more complete comparison of the theory with results at these frequencies.

¹⁾Kuybyshev State University

¹Y. Kagawa, T. Hatakeyama, and Y. Tanaka, *J. Sound and Vibr.* **41**, 1, (1975).

²H. Bruchmüller, *Acustica* **40**, 155 (1978).

³O. A. Kapustina, E. N. Kozhevnikov, and G. N. Yakovenko, in: Abstracts, 4th Conf. of Socialist Countries on Liquid Crystals, Vol. 2, Tbilisi, 1981, p. 62.

⁴E. Dubois-Violette and F. Rothen, *J. de Phys.* **39**, 1039 (1978).

⁵M. J. Stephen and J. P. Straley, *Rev. Mod. Phys.* **46**, 617 (1974).

⁶M. Born and E. Wolf, *Principles of Optics*, Pergamon, 1970.

⁷Yu. N. Korolev and G. N. Yakovenko, *Akust. Zh.* **23**, No. 5, 783 (1977) [*Sov. Phys. Acoustics* **23**, 447 (1977)].

⁸S. Naemura, *Appl. Phys. Lett.* **33**, 1 (1978).

⁹O. A. Kapustina, E. N. Kozhevnikov, and G. J. Jakovenko, in: Abstracts, 11 Intern. Congres d'Acoustique, Paris, 183, Vol. 2, p. 77.

Translated by J. G. Adashko